Table S1: Linear regression results for total measured anion and cation concentrations in precipitation at selected sites

Sampling period	Site	Site setting	Slope	Intercept	R^2	Reference
2023	ABLES, Zhejiang, China	Mountain	0.39	6.43	0.96	This study
2000–2001	Tirupati, India	Urban	0.71	59.91	0.92	Chandra Mouli et al., 2005
2007	Dandong, China	Urban	1.03	-20.16	0.94	Ge et al., 2016
2007	Dalian, China	Urban	0.95	1.98	0.92	Ge et al., 2016
2014	Beijing, China	Urban	0.75	3.47	0.95	Xu et al., 2017
2011–2016	Shanghai, China	Urban	0.95	0.23	0.93	Meng et al., 2019
2017–2018	Beijing (Yanqing), China	Rural	0.96	—	0.98	Xu et al., 2020
2005–2006	Nam Co, Tibetan Plateau	Remote mountain	0.78	—	0.93	Li et al., 2007
2005–2009	Nam Co, Tibetan Plateau	Remote mountain	0.37	—	—	Zhang et al., 2012
2009	Mangdang Mountain, China	Mountain	0.38	—	0.92	Cheng et al., 2011
2009–2010	Southeastern Tibetan Plateau	Mountain	0.97	5.59	0.95	Liu et al., 2013
2012–2013	Central Qilian Mountains, China	Mountain	0.21	0.21	0.56	Li et al., 2015
2011–2012	Kathmandu, Nepal	Urban	0.44	-9.26	0.74	Tripathee et al., 2014
2011–2012	Dhunche, Nepal	Rural mountain	0.43	-1.29	0.83	Tripathee et al., 2014
2011–2012	Dimsa, Nepal	Remote mountain	0.49	3.28	0.92	Tripathee et al., 2014
2011–2012	Gosainkunda, Nepal	Remote mountain	0.48	3.10	0.89	Tripathee et al., 2014

Note: The fitted relationship is $\Sigma A = \text{slope} \times \Sigma C + \text{intercept}$, where ΣA and ΣC are the total measured anion and cation equivalent concentrations, respectively. Intercepts are reported in $\mu eq\ L^{-1}$. "—" indicates that a value was not reported.

Table S2: Summary statistics for major ions in precipitation at ABLES during the 2023 observation period (unit: μeq L^{-1}).

Statistic	F^-	Cl^-	NO_3^-	SO_4^{2-}	NH_4^+	Mg^{2+}	K^+	Ca^{2+}	Na^+
VWM	4	10	6	14	23	4	9	22	11
Arithmetic mean	5	10	7	10	31	9	3	16	13
Median	5	8	5	7	20	9	2	11	10
Maximum	21	72	55	73	247	142	16	68	147
Minimum	0	0	0	0	0	0	1	1	0
SD	4	9	7	11	37	11	2	14	14

Table S3: Comparison of major ion concentrations in precipitation at ABLES and selected background, mountain, and urban sites (unit: μeq L^{-1}).

Site	Type	Period	F^-	Cl^-	NO_3^-	SO_4^{2-}	NH_4^+	Mg^{2+}	K^+	Ca^{2+}	Na^+	Σ8	Reference
ABLES (SH)	Mountain	2023	4	10	6	14	23	4	9	22	11	99	This study
Waliguan (WLG)	Background	2018	4.3	21	24.6	52.9	37.1	19.7	5.8	175.4	28.3	364.8	Jia et al., 2019
Shangdianzi (SDZ)	Background	2018	2.6	7.7	49.4	51.9	107.2	11.5	1.8	70.4	4.4	304.3	Jia et al., 2019
Lin'an (LN)	Background	2018	1.6	7.8	33.7	30.4	37.1	5	1	50.9	3.3	169.2	Jia et al., 2019
Longfengshan (LFS)	Background	2018	1.7	9.2	29.1	33.4	46.5	8	6.2	57.3	14.2	203.9	Jia et al., 2019
Jinsha (JS)	Background	2018	3.2	21.1	47.1	68.6	35.7	16.1	15.4	134.5	18.3	356.8	Jia et al., 2019
Maolan forest	Background	2007–2008	0.9	5.14	3.01	40.35	30.21	3.03	3.5	20.84	2.35	108.43	Han et al., 2010
West Virginia, USA	Mountain	2000–2014	—	4	29	13	16	1	1	4	3	71	Andronache, 2016
Nam Co	Mountain	2005	—	0	0	2	1	0	0	5	1	9	Li et al., 2007
Nanping Mountain, Fujian	Mountain	2009	1	6	27	37	38	5	5	26	5	149	Cheng et al., 2011
Tibetan Plateau	Mountain	2009–2010	—	7	2	3	9	2	2	34	7	66	Liu et al., 2013
Jiuzhaigou	Mountain	2011	21	37	13	71	13	21	41	150	38	384	Qiao et al., 2015
Kathmandu, Nepal	Mountain	2011–2012	—	5	13	16	48	2	5	39	4	132	Tripathee et al., 2014
Dhunche, Nepal	Mountain	2011–2013	—	5	11	10	27	2	3	25	4	87	Tripathee et al., 2014
Dimsa, Nepal	Mountain	2011–2014	—	23	9	8	23	4	6	19	21	113	Tripathee et al., 2014
Gosainkunda, Nepal	Mountain	2011–2015	—	15	4	7	20	4	3	10	11	74	Tripathee et al., 2014
Ganhaizi Basin	Mountain	2012	1	2	4	28	13	2	6	38	4	97	Niu et al., 2014
Lijiang	Mountain	2012	1	2	7	24	21	2	11	50	1	118	Niu et al., 2014
Mt Everest, Nepal	Mountain	2013	—	2	2	1	5	0	0	4	1	15	Balestrini et al., 2016
Qilian Mountains	Mountain	2013	—	20	47	18	—	9	34	132	23	≥283	Li et al., 2015
Mt Åreskutan, Sweden	Mountain	2014	—	7	11	9	9	2	2	17	7	64	Vega et al., 2019
Mt Emei	Mountain	2017–2019	1	6	18	26	43	3	2	15	3	116	Zhang et al., 2020
Southeast Tibet Station	Mountain	2011–2012	—	2.5	2.2	2.1	4.9	0.9	1	20.8	3.8	38.2	Liu et al., 2015
Qomolangma Station (China)	Mountain	2011–2012	—	27.1	0.8	3.2	25.4	1.7	4.5	53.4	26	142.1	Liu et al., 2015
Ngari Station	Mountain	2013	—	11.9	4.8	11.6	20.5	4.8	1.8	50.9	12.4	118.7	Liu et al., 2015
Muztagh Ata Station	Mountain	2011	—	8.9	9.9	17.4	42	11.3	3	119.4	10.1	222	Liu et al., 2015
Eastern Tien Shan alpine site	Mountain	2003–2004	—	16.5	9.6	53	25.2	18.1	4	174.2	19	319.6	Zhao et al., 2008
Tirupati, India	Urban	2000	5	34	41	128	20	34	56	151	33	497	Chandra Mouli et al., 2005
Chongqing	Urban	2003–2013	—	17	47	104	97	10	4	56	11	346	Liu et al., 2016
Sichuan	Urban	2011–2016	10	20	60	201	75	12	25	139	24	556	Li et al., 2019
Beijing	Urban	2014	5	15	91	162	240	18	5	65	10	606	Xu et al., 2017
Jiaozhou	Urban	2015–2016	3	66	63	94	107	17	22	64	55	488	Xing et al., 2017
Shanghai	Urban	2016	4	19	41	60	68	3	7	32	16	246	Meng et al., 2019
Beijing	Urban	2017	—	123	70	77	90	74	24	130	69	657	Xu et al., 2020
Beijing	Urban	2018	—	77	49	55	63	38	42	152	49	525	Xu et al., 2020
Beijing	Urban	2021	4	22	72	55	192	6	25	41	17	430	Zeng et al., 2022
Guiyang	Urban	2022–2023	8	9	27	50	58	10	6	71	8	239	Zeng et al., 2024a
Chengdu	Urban	2008	6.2	8.9	156.2	212.8	150.5	16.2	6.6	196.6	1.4	749.2	Wang and Han, 2011
Xi'an	Urban	Mar–May 2010	28.7	38.7	128.8	489.7	229.8	36.6	13.8	425.6	31.1	1394.1	Lu et al., 2011
Shenzhen	Urban	2005–2009	1.72	20.6	21.9	64.7	33.5	3.26	1.75	35.4	11.2	192.31	Huang et al., 2010
Nanjing	Urban	1992–2003	19.1	142.6	39.6	241.8	193.2	31.7	12.1	295.4	23	979.4	Tu et al., 2005
Hangzhou	Urban	2006–2008	—	13.9	38.4	110	79.9	7.1	4.2	51.9	12.2	317.6	Xu et al., 2011

Note: Σ8 is the sum of Cl^-, NO_3^-, SO_4^{2-}, NH_4^+, Mg^{2+}, K^+, Ca^{2+}, and Na^+; F^- is excluded so that sites without reported F^- remain comparable. An em dash indicates that a value was not reported. For the Qilian Mountains, NH_4^+ was not reported; therefore, Σ8 is shown as a lower bound (≥283 μeq L^{-1}).

Table S4: Arithmetic mean concentrations of each event's final three sequential fractions for rainfall events R1–R12

Event	SO_4^{2-} (mg L^{-1})	NO_3^- (mg L^{-1})	NH_4^+ (mg L^{-1})	Na^+ (mg L^{-1})	Cl^- (mg L^{-1})	F^- (mg L^{-1})	K^+ (mg L^{-1})	Mg^{2+} (mg L^{-1})	Ca^{2+} (mg L^{-1})
R1	0.61	0.24	0.36	0.19	0.11	0.12	0.22	0.12	0.10
R2	0.53	0.18	0.17	0.33	0.04	0.08	0.36	0.04	0.44
R3	1.24	0.59	1.13	0.22	0.36	0.15	0.47	0.05	0.51
R4	1.00	0.38	0.83	0.27	0.34	0.24	0.42	0.05	0.55
R5	0.05	0.19	0.03	0.20	0.22	0.06	0.35	0.03	0.22
R6	0.12	0.21	0.07	0.21	0.30	0.06	0.37	0.04	0.46
R7	0.46	0.21	0.08	0.30	0.33	0.07	0.38	0.05	0.50
R8	0.60	0.27	0.33	0.23	0.40	0.10	0.39	0.05	0.45
R9	0.68	0.28	0.21	0.31	0.50	0.06	0.25	0.09	1.42
R10	0.35	0.15	0.10	0.46	0.52	0.04	0.26	0.07	1.87
R11	0.43	0.20	0.17	0.46	0.53	0.04	0.27	0.06	1.35
R12	0.16	0.06	0.01	0.01	0.01	0.01	0.02	0.03	0.18

Note: Values are arithmetic mean concentrations calculated from each event's final three valid sequential rainwater fractions.

Table S5a: Rotated component loadings of the nine measured ions and source-related interpretation at ABLES.

Ion	Rotated loading		
	PC1	**PC2**	**PC3**
F^-	0.244	0.177	0.051
Cl^-	0.184	**0.854**	0.318
NO_3^-	**0.867**	0.234	0.334
SO_4^{2-}	**0.719**	0.246	0.476
NH_4^+	**0.805**	0.183	0.375
K^+	**0.869**	0.421	0.113
Mg^{2+}	0.667	0.448	**0.499**
Ca^{2+}	0.337	0.268	**0.878**
Na^+	0.541	**0.781**	0.139
Rotated variance explained (%)	40.2	21.9	18.2
Cumulative rotated variance (%)	40.2	62.1	80.3
Source type	Anthropogenic source	Sea salt source	Crustal source

Note: Bold values indicate the dominant loadings used for component interpretation. The first three rotated components explained 80.2% of the total variance and were retained for source-related interpretation.

Table S5b: Pearson correlation coefficients among major ions in precipitation at ABLES.

Ion	F^-	NO_3^-	SO_4^{2-}	Cl^-	NH_4^+	K^+	Ca^{2+}	Na^+	Mg^{2+}
F^-	1.000								
NO_3^-	0.475**	1.000							
SO_4^{2-}	0.553**	0.903**	1.000						
Cl^-	0.423**	0.541**	0.614**	1.000					
NH_4^+	0.565**	0.962**	0.955**	0.557**	1.000				
K^+	0.403**	0.895**	0.789**	0.560**	0.818**	1.000			
Ca^{2+}	0.234	0.652**	0.701**	0.533**	0.632**	0.532**	1.000		
Na^+	0.366**	0.708**	0.663**	0.771**	0.642**	0.813**	0.554**	1.000	
Mg^{2+}	0.456**	0.876**	0.890**	0.719**	0.858**	0.863**	0.774**	0.761**	1.000

Note: Values are Pearson's correlation coefficients calculated from 55 rainfall events. ** $p < 0.01$ (two-tailed). Blank cells in the upper triangle are omitted to avoid duplication.

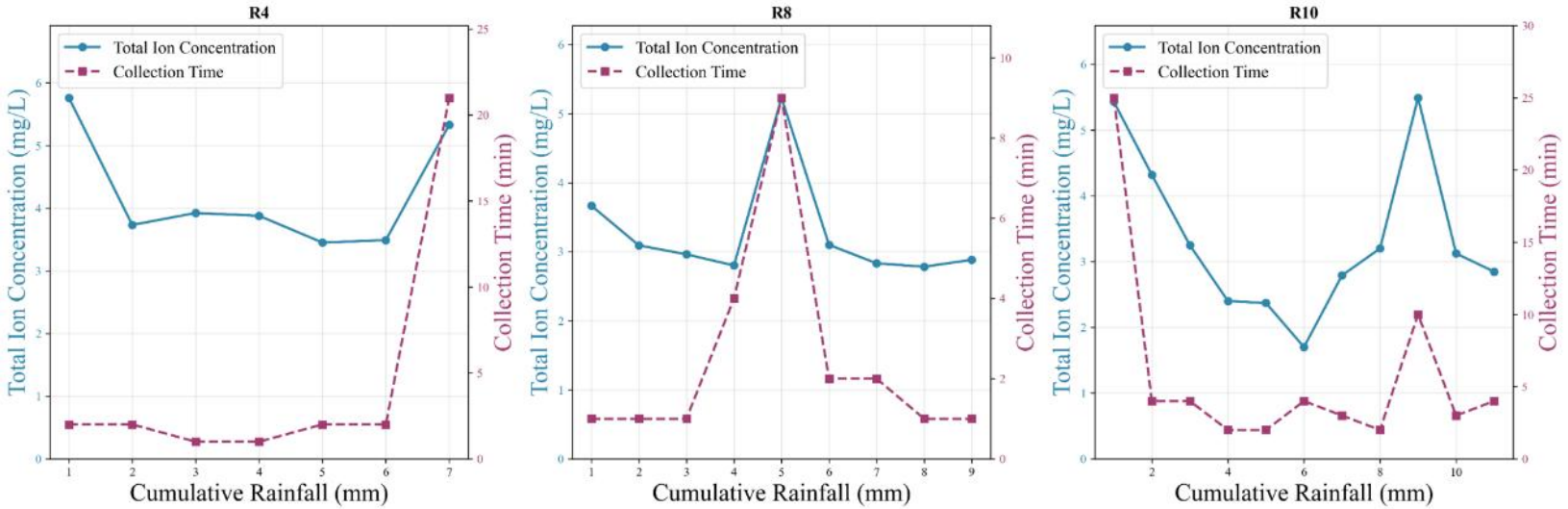


Figure S1: Variations in total ion concentration and collection time with cumulative rainfall during events R4, R8, and R10. Blue solid lines represent the total concentration of the nine measured ions, and magenta dashed lines represent the collection time of each sequential rainwater fraction. Total ion concentration and collection time correspond to the left and right y-axes, respectively. Because successive fractions represented approximately equal rainfall depths, a longer collection time generally indicates a lower average rainfall intensity during the corresponding fraction.

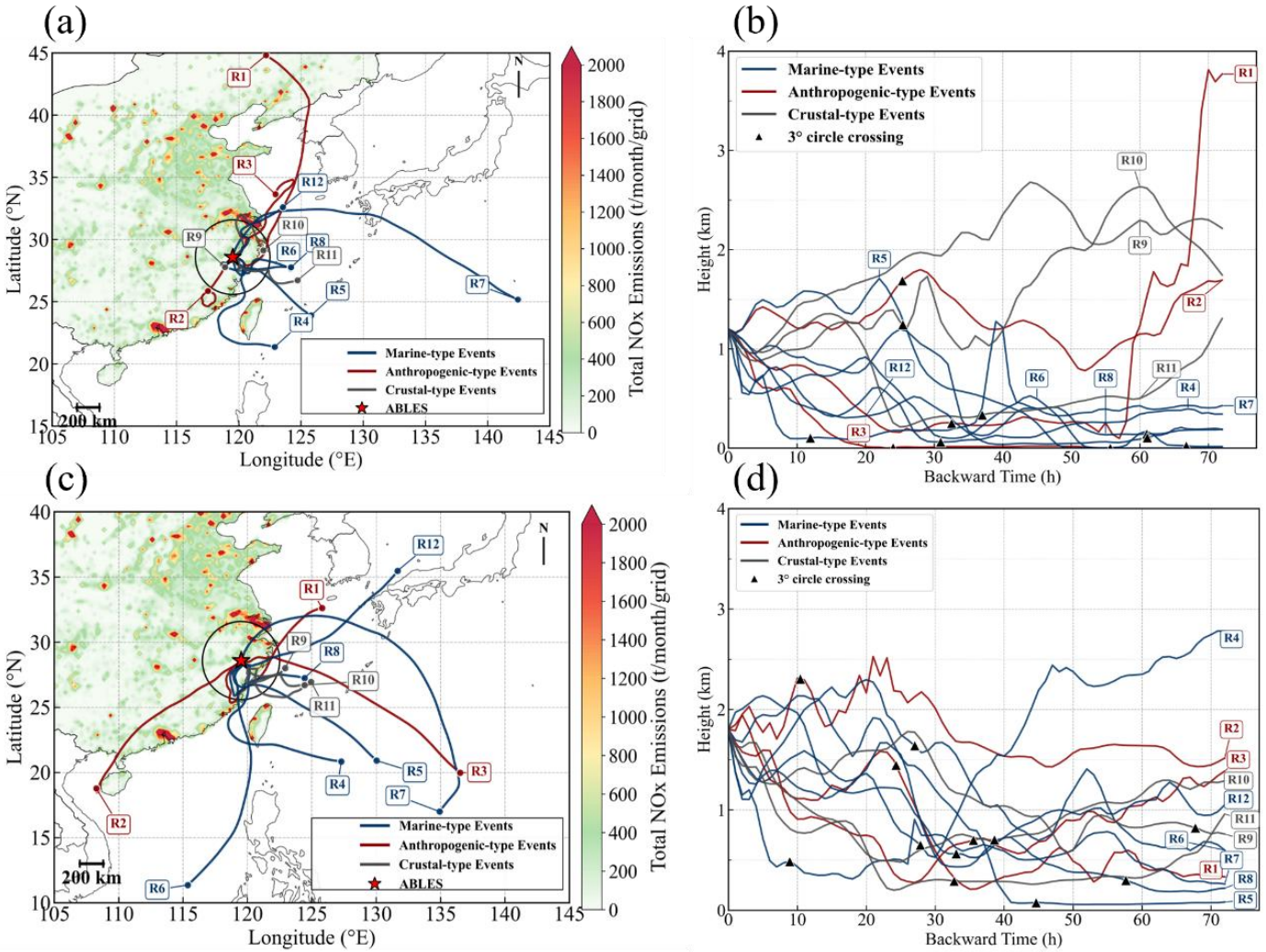


Figure S2: Seventy-two-hour backward trajectories and corresponding height profiles for the 12 sequentially sampled rainfall events at ABLES. Trajectories arrived at ABLES at (a, b) 1200 m a.s.l. and (c, d) 1800 m a.s.l. Panels (a) and (c) show the trajectories superimposed on monthly total NO_x emissions, whereas panels (b) and (d) show trajectory height as a function of backward time. Blue, red, and gray lines represent marine-, anthropogenic-, and crustal-type events, respectively. The red star marks ABLES, the black circle indicates the 3° radius around the site, and black triangles indicate the positions at which the trajectories crossed this circle. R1–R12 denote the individual rainfall events.

References

Andronache, C.: Dependence of daily aerosol wet deposition on precipitation at Appalachian Mountains site in the United States, Aerosol Air Qual. Res., 16, 665–673, https://doi.org/10.4209/aaqr.2015.05.0322, 2016.

Balestrini, R., Delconte, C. A., Sacchi, E., Wilson, A. M., Williams, M. W., Cristofanelli, P., and Putero, D.: Wet deposition at the base of Mt Everest: Seasonal evolution of the chemistry and isotopic composition, Atmos. Environ., 146, 100–112, https://doi.org/10.1016/j.atmosenv.2016.08.056, 2016.

Chandra Mouli, P., Venkata Mohan, S., and Jayarama Reddy, S.: Rainwater chemistry at a regional representative urban site: influence of terrestrial sources on ionic composition, Atmos. Environ., 39, 999–1008, https://doi.org/10.1016/j.atmosenv.2004.10.036, 2005.

Cheng, Y., Liu, Y., Huo, M., Sun, Q., Wang, H., Chen, Z., and Bai, Y.: Chemical characteristics of precipitation at Nanping Mangdang Mountain in eastern China during spring, J. Environ. Sci., 23, 1350–1358, https://doi.org/10.1016/S1001-0742(10)60560-8, 2011.

Ge, B., Wang, Z., Gbaguidi, A. E., and Zhang, Q.: Source identification of acid rain arising over Northeast China: observed evidence and model simulation, Aerosol Air Qual. Res., 16, 1366–1377, https://doi.org/10.4209/aaqr.2015.05.0294, 2016.

Han, G., Tang, Y., Wu, Q., and Tan, Q.: Chemical and strontium isotope characterization of rainwater in karst virgin forest, Southwest China, Atmos. Environ., 44, 174–181, https://doi.org/10.1016/j.atmosenv.2009.10.019, 2010.

Huang, X.-F., Li, X., He, L.-Y., Feng, N., Hu, M., Niu, Y.-W., and Zeng, L.-W.: 5-Year study of rainwater chemistry in a coastal mega-city in South China, Atmos. Res., 97, 185–193, https://doi.org/10.1016/j.atmosres.2010.03.027, 2010.

Jia, X., Tang, J., and Zhang, Y.: The precipitation chemistry and acidity over China during 2018, E3S Web Conf., 136, 06020, https://doi.org/10.1051/e3sconf/201913606020, 2019.

Li, C., Kang, S., Zhang, Q., and Kaspari, S.: Major ionic composition of precipitation in the Nam Co region, Central Tibetan Plateau, Atmos. Res., 85, 351–360, https://doi.org/10.1016/j.atmosres.2007.02.006, 2007.

Li, J., Li, R., Cui, L., Meng, Y., and Fu, H.: Spatial and temporal variation of inorganic ions in rainwater in Sichuan province from 2011 to 2016, Environ. Pollut., 254, 112941, https://doi.org/10.1016/j.envpol.2019.07.109, 2019.

Li, Z., Li, Z., Wang, T., Gao, Y., Cheng, A., Guo, X., Guo, R., Jia, B., Song, Y., Han, C., and Theakstone, W. H.: Composition of wet deposition in the central Qilian Mountains, China, Environ. Earth Sci., 73, 7315–7328, https://doi.org/10.1007/s12665-014-3907-0, 2015.

Liu, B., Kang, S., Sun, J., Zhang, Y., Xu, R., Wang, Y., Liu, Y., and Cong, Z.: Wet precipitation chemistry at a high-altitude site (3,326 m a.s.l.) in the southeastern Tibetan Plateau, Environ. Sci. Pollut. Res., 20, 5013–5027, https://doi.org/10.1007/s11356-012-1379-x, 2013.

Liu, L., Zhang, X., and Lu, X.: The composition, seasonal variation, and potential sources of the atmospheric wet sulfur (S) and nitrogen (N) deposition in the southwest of China, Environ. Sci. Pollut. Res., 23, 6363–6375, https://doi.org/10.1007/s11356-015-5844-1, 2016.

Liu, Y. W., Xu-Ri, Wang, Y. S., Pan, Y. P., and Piao, S. L.: Wet deposition of atmospheric inorganic nitrogen at five remote sites in the Tibetan Plateau, Atmos. Chem. Phys., 15, 11683–11700, https://doi.org/10.5194/acp-15-11683-2015, 2015.

Lu, X. W., Li, L. Y., Li, N., Yang, G., Luo, D. C., and Chen, J. H.: Chemical characteristics of spring rainwater of Xi'an city, NW China, Atmos. Environ., 45, 5058–5063, https://doi.org/10.1016/j.atmosenv.2011.06.026, 2011.

Meng, Y., Zhao, Y., Li, R., Li, J., Cui, L., Kong, L., and Fu, H.: Characterization of inorganic ions in rainwater in the megacity of Shanghai: spatiotemporal variations and source apportionment, Atmos. Res., 222, 12–24, https://doi.org/10.1016/j.atmosres.2019.01.023, 2019.

Niu, H., He, Y., Lu, X. X., Shen, J., Du, J., Zhang, T., Pu, T., Xin, H., and Chang, L.: Chemical composition of rainwater in the Yulong Snow Mountain region, Southwestern China, Atmos. Res., 144, 195–206, https://doi.org/10.1016/j.atmosres.2014.03.010, 2014.

Qiao, X., Xiao, W., Jaffe, D., Kota, S. H., Ying, Q., and Tang, Y.: Atmospheric wet deposition of sulfur and nitrogen in Jiuzhaigou National Nature Reserve, Sichuan Province, China, Sci. Total Environ., 511, 28–36, https://doi.org/10.1016/j.scitotenv.2014.12.028, 2015.

Tripathee, L., Kang, S., Huang, J., Sillanpää, M., Sharma, C. M., Lüthi, Z. L., Guo, J., and Paudyal, R.: Ionic composition of wet precipitation over the southern slope of central Himalayas, Nepal, Environ. Sci. Pollut. Res., 21, 2677–2687, https://doi.org/10.1007/s11356-013-2197-5, 2014.

Tu, J., Wang, H. S., Zhang, Z. F., Jin, X., and Li, W. Q.: Trends in chemical composition of precipitation in Nanjing, China, during 1992–2003, Atmos. Res., 73, 283–298, https://doi.org/10.1016/j.atmosres.2004.11.002, 2005.

Vega, C. P., Mårtensson, E. M., Wideqvist, U., Kaiser, J., Zieger, P., and Ström, J.: Composition, isotopic fingerprint and source attribution of nitrate deposition from rain and fog at a Sub-Arctic Mountain site in Central Sweden (Mt Åreskutan), Tellus B, 71, 1559398, https://doi.org/10.1080/16000889.2018.1559398, 2019.

Wang, H. and Han, G.: Chemical composition of rainwater and anthropogenic influences in Chengdu, Southwest China, Atmos. Res., 99, 190–196, https://doi.org/10.1016/j.atmosres.2010.10.004, 2011.

Xing, J., Song, J., Yuan, H., Li, X., Li, N., Duan, L., Qu, B., Wang, Q., and Kang, X.: Chemical characteristics, deposition fluxes and source apportionment of precipitation components in the Jiaozhou Bay, North China, Atmos. Res., 190, 10–20, https://doi.org/10.1016/j.atmosres.2017.02.001, 2017.

Xu, D., Ge, B., Wang, Z., Sun, Y., Chen, Y., Ji, D., Yang, T., Ma, Z., Cheng, N., Hao, J., and Yao, X.: Below-cloud wet scavenging of soluble inorganic ions by rain in Beijing during the summer of 2014, Environ. Pollut., 230, 963–973, https://doi.org/10.1016/j.envpol.2017.07.033, 2017.

Xu, H., Bi, X.-H., Feng, Y.-C., Lin, F.-M., Jiao, L., Hong, S.-M., Liu, W.-G., and Zhang, X.-Y.: Chemical composition of precipitation and its sources in Hangzhou, China, Environ. Monit. Assess., 183, 581–592, https://doi.org/10.1007/s10661-011-1963-4, 2011.

Xu, W., Wen, Z., Shang, B., Dore, A. J., Tang, A., Xia, X., Zheng, A., Han, M., Zhang, L., Zhao, Y., Zhang, G., Feng, Z., Liu, X., and Zhang, F.: Precipitation chemistry and atmospheric nitrogen deposition at a rural site in Beijing, China, Atmos. Environ., 223, 117253, https://doi.org/10.1016/j.atmosenv.2019.117253, 2020.

Zeng, J., Han, G., Wu, Q., Peng, M., Ge, X., Mao, S., Wang, Z., and Ma, Q.: Chemical evolution of rainfall in China's first eco-civilization demonstration city: Implication for the provenance identification of pollutants and rainwater acid neutralization, Sci. Total Environ., 910, 168567, https://doi.org/10.1016/j.scitotenv.2023.168567, 2024a.

Zeng, J., Han, G., Zhang, S., Xiao, X., Li, Y., Gao, X., Wang, D., and Qu, R.: Rainwater chemical evolution driven by extreme rainfall in megacity: Implication for the urban air pollution source identification, J. Clean. Prod., 372, 133732, https://doi.org/10.1016/j.jclepro.2022.133732, 2022.

Zhang, Y., Cao, Y., Tang, Y., Ying, Q., Hopke, P. K., Zeng, Y., Xu, X., Xia, Z., and Qiao, X.: Wet deposition of sulfur and nitrogen at Mt. Emei in the West China Rain Zone, southwestern China: Status, inter-annual changes, and sources, Sci. Total Environ., 713, 136676, https://doi.org/10.1016/j.scitotenv.2020.136676, 2020.

Zhang, Y., Kang, S., Li, C., Cong, Z., and Zhang, Q.: Wet deposition of precipitation chemistry during 2005–2009 at a remote site (Nam Co Station) in central Tibetan Plateau, J. Atmos. Chem., 69, 187–200, https://doi.org/10.1007/s10874-012-9236-3, 2012.

Zhao, Z., Tian, L., Fischer, E., Li, Z., and Jiao, K.: Study of chemical composition of precipitation at an alpine site and a rural site in the Urumqi River Valley, Eastern Tien Shan, China, Atmos. Environ., 42, 8934–8942, https://doi.org/10.1016/j.atmosenv.2008.08.003, 2008.